Jordan Journal of Civil Engineering, Volume **17**, No. **4**, **2023**
DOI: https://doi.org/10.14525/JJCE.v17i4.14

Machine Vision Based The Spatiotemporal Information Identification of The Vehicle

Chao Wang [1)*], ***Gui-Ning Han*** [2)], ***Tian-Yu Qi*** [3)] ***and Qing-Xiang Yang*** [4)]

[1) 1),2),3),4)] School of Civil Engineering, Architecture and Environment, Key Laboratory of Health Intelligent Perception and Ecological Restoration of River and Lake, Ministry of Education, Hubei University of Technology, Wuhan 430068, China. * Corresponding Author. E-Mail: cwang@hbut.edu.cn

ABSTRACT

Accurately identifying the vehicle load on the bridge plays a vital role in structural-stress analysis and safety evaluation. Also, extracting the spatiotemporal information of the vehicle's is crucial for identifying the vehicle load. This study aimed to propose a vehicle spatiotemporal information-identification method based on machine-vision technology. First, digital video surveillance cameras were installed in the front and on the side of the monitoring section to capture real-time videos of vehicles passing through the monitoring section. The background-difference method was used to detect vehicles based on the frontal video. Subsequently, the transverse position was evaluated according to the distance between the vehicle's license plate and the lane line. Other vehicle parameters, including the vehicle's speed, the number of axles and the wheelbase, were identified based on the lateral video and the auxiliary lines with a known distance. Second, a laboratory model experiment and multiple field tests under different scenes were carried out to validate the efficiency and accuracy of the proposed method. The results indicated that the average identification errors of wheelbase for the model experiment and the field tests were all 1.12% and those of the vehicle's speed were 1.25% and 1.35, respectively. Also, the average deviations of the lateral position were 2.57 mm and 2.69 cm, respectively. The variances of the identified error of the three parameters for the field tests were 0.78%, 1.83 cm and 0.54%, respectively. This verified that the proposed method has high accuracy, reliability and good anti-noise performance.

KEYWORDS: Machine vision, Spatiotemporal information, Load identification, Orthotropic deck, Bridge engineering.

INTRODUCTION

The orthotropic-deck steel box girder structure is widely used in large-span bridges. However, the local stress of the deck is highly prominent. The vehicle load is the main variable load. Therefore, accurately acquiring the vehicle load, including spatiotemporal information and weight of the vehicle, for the structural fatigue analysis and performance evaluation, is essential (Li et al., 2022; Sujon and Dai, 2021; Zhang et al., 2019). Currently, the main identifying methods are based on structural dynamics response and weigh-in-motion (WIM). The former class of methods solves the interaction force between the vehicle and the bridge based on the theory of a one-dimensional beam (Wen et al., 2021; Miao et al., 2018; Yang et al., 2016). Zhu et al (2021) proposed a two-step solution for real-time vehicle identification designed for acceleration measurements. A sequence-to-label long–short-term memory (LSTM) network is constructed to identify axle-induced responses in a multilane system directly. Considering the influence of the transverse distribution of the vehicle load in a two-dimensional deck, which holds great importance for the orthotropic-deck steel box girder structure, accurately assessing its influence can be quite challenging. The method based on WIM identified vehicle load according to the relationship between strain response and vehicle load (Zhao et al., 2019; Obrien and Enright, 2012; Han et al., 2018). Due

Received on 10/2/2023.
Accepted for Publication on 15/8/2023.

to the prominent local force in an orthotropic deck, the variation in the spatial position of the vehicle on the bridge deck affects the identification of the vehicle load (Yang et al., 2012). Therefore, determining the transverse position based on the conjoint analysis of multiple sensor data is essential. Also, the known vehicle load on different transverse positions on the deck should be known to calibrate the structural strain response. Zhu et al. (2022) proposed a cosine similarity index to locate the transverse position of the vehicle. An optimal combined strain influence line was developed using a genetic algorithm to decrease the influence of the transverse position of the load (Li et al., 2022). However, precisely locating the transverse position can be a challenging task on site. Additionally, the WIM method needs to identify the vehicle's speed, the number of axles and the wheelbase to accurately assess the vehicle load. Deng et al. (2018) proposed the equivalent shear force method to detect the speed and axles of moving vehicles. He et al. (2019) adopted the virtual-axle method to detect the axles. The wavelet-transform method was proposed to identify the vehicle axles by Zhao et al. (2016) and Wang et al. (2013). Xiao et al. (2006) and Yamaguchie et al. (2009) introduced the shearing-strain method to identify the vehicle axles. These methods are generally applied to specific bridges and need to install many sensors in multi-monitoring sections.

Machine-vision technology is a non-contact monitoring technology without additional sensors, which does not affect traffic. Many scholars recently adopted this technology to monitor infrastructure (Wang et al., 2022; Jiang et al., 2022). Mohammed (2020) developed an expert system that helps people perform a safe roadway crossing through video cameras. Mohammed and Tasneem (2022) used the captured images by cellular phones' cameras to extract some of traffic-monitoring parameters as well as road inventory, vehicle classification and intersections. A computer-vision cellular-phone based system was proposed to extract traffic and pedestrian parameters (Mohammed et al., 2022). Machine-vision technology has also provided a method for directly monitoring vehicle load. Chen et al (2020) proposed a non-contact vehicle-identification methodology to distinguish a vehicle from its load based on machine-vision technology and deep-learning algorithms. Binocular-vision technology was used to continuously track the spatial position of the vehicle (Zhao et al., 2021). Chen et al. (2013) used a dynamic image-identification technique to obtain the transverse vehicle distribution. Ryan and Al (2016) proposed a position-identification method based on the background-foreground segment technique. Chen et al. (2016) adopted machine-vision technology to obtain the spatiotemporal distribution of traffic vehicles on the bridge. Khuc and Catbas (2018) identified the vehicle's speed and axle information based on the traffic-flow video.

This study proposed a vehicle spatiotemporal information-identification method based on machine-vision technology. The digital video surveillance cameras were installed in the front and on the side of the monitoring section to capture videos of vehicles passing through the monitoring section. Firstly, the frontal video was decomposed into a sequence of image frames and the moving vehicle was detected based on the background-difference technique. In the following, the license plate was located using the rectangular pattern-matching method and the lane lines were extracted using the progressive probabilistic Hough transform algorithm. Based on the distance between the license plate and the lane lines, the transverse position of the vehicle could be located. Secondly, the lateral video was processed to identify wheels using the standard circle Hough transform technique and transverse auxiliary detection lines with known distance were detected using the same method as the lane lines' detection. Therefore, the wheelbase could be estimated based on the relative distance between the wheels and the auxiliary lines and the vehicle's speed was identified according to the difference position of the same wheel in different frame images.

The rest of this article was organized as follows: First, the proposed identification method of the transverse position, axles and vehicle's speed was introduced. Then, laboratory model experiment and field tests under different scenes were carried out to validate the efficiency and accuracy of the proposed method. Finally, several conclusions are drawn.

Identification Method

The high-frame rate digital video surveillance cameras are installed in the front and on the sides of the monitoring section to capture the traffic-flow video so

as to monitor the vehicles' spatiotemporal information on the bridge. The frontal video obtained using the camera was used to locate the transverse position, whereas the lateral video was used to evaluate the vehicle's speed, number of axles and wheelbase. The whole theoretical framework is shown in Fig. 1.

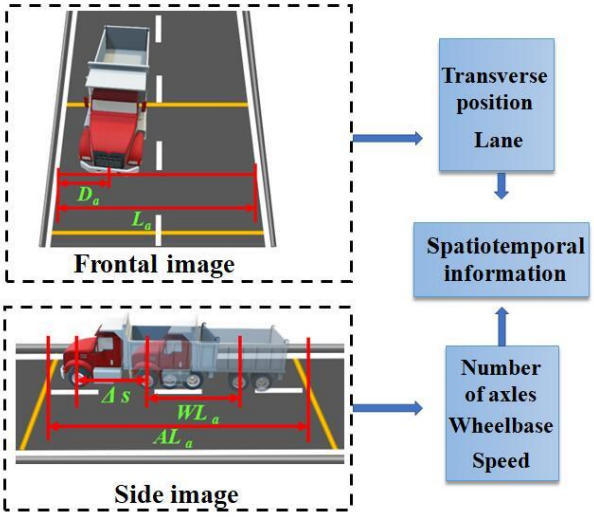

Figure (1): Spatiotemporal information-identification framework

Vehicle Detection

The cameras are static and the shooting angle is constant. Hence, whether a vehicle enters the monitoring region from the video needs to be detected. In this study, the background-difference technique (Zhou, 2018) was adopted for vehicle detection in the video stream data captured by the camera. The main idea involves decomposing the video into a sequence of video image frames and subsequently identifying the changing target in each frame of the image to identify the moving vehicle.

First, the background model needed to be built based on video frames without the vehicle. The color images of video frames were extracted from the front camera and converted into grayscale images. The background model was built by the multi-frame averaging method, as shown in Eq. (1):

$$B_k(x,y) = \frac{1}{N}\sum_{k=1}^{N} J_k(x,y) \tag{1}$$

where B_k is the background model in the k^{th} frame image, N is the total number of image frames and $J_k(x,y)$. is the image composed of all the pixels in the k^{th} frame image.

The background is updated at regular intervals to eliminate the influence of illumination, as shown in the following equation:

$$B_k = B_{k-1} + \frac{1}{N}\left(J_k - J_{k\_N}\right). \tag{2}$$

We acquired the foreground grayscale image of the current frame by subtracting the obtained background image $B_k(x,y)$ from the grayscale image $P_k(x,y)$. The resulting image was binary processed to the foreground image $O(x,y)$:

$$O(x,y) = \begin{cases} 1, \left|P_k(x,y) - B_k(x,y)\right| \geq \mathrm{T} \\ 0, \left|P_k(x,y) - B_k(x,y)\right| < \mathrm{T} \end{cases} \tag{3}$$

where T is the threshold of binarization. It was determined using the Otsu method (Kim et al., 2009). For an image $C_k(x,y)$, the proportion of the pixels belonging to the foreground is denoted as ω_0 and its average gray level is μ_0; the ratio of background pixels is expressed as ω_1 and its average gray level is μ_1. Therefore, the inter-class variance between the foreground and the background was calculated as follows:

$$\sigma = \omega_0 \bullet \omega_1 \bullet (\mu_0 - \mu_1)^2. \tag{4}$$

The optimal threshold T should maximize the inter-class variance δ, which was obtained by the traversal method.

Whether a vehicle enters the monitoring region was detected based on the difference between the foreground and the background.

Identification of the Transverse Position

After the vehicle was detected, the corresponding image frame containing the moving vehicle was isolated and converted into grayscale. The subsequent step involves identifying the license plate and lane lines within the frame to locate the transverse position of the vehicle. First, the license plate was located by the rectangular pattern-matching method. Some parts with similar shapes, such as automotive lamps and reflective mirrors, were also identified. Hence, the mean shift (MS) clustering algorithm (Jia et al., 2019) was adopted to split the image into different parts.

Assuming a feature space with a center point x_0 was

initially set and all vectors composed by the center point and all points in the circular area with a radius of *h* were calculated. Then, we obtained an MS by calculating the average value of all vectors:

$$MS(x) = \frac{1}{k} \bullet \sum_{x_i \in S_h} (x_i - x_0) \tag{5}$$

Where S_h is a high-dimensional spherical region with a center point x_0 and radius h, x_i is the point in the range of S_h and k is the number of all points.

After the MS was obtained, the center point was moved to the new point along the shift vector. The new MS was calculated until the shift was small enough and all the other points were determined using the same calculation. Therefore, the image was divided into different parts.

Considering the characters on the license plate, the pixel values of the license plate region usually have a higher local variance. Therefore, we could accurately locate the license plate by calculating the edge density of the candidate area:

$$W_R = \frac{1}{N_R} \sum_{m,n \in R} E(m,n) \tag{6}$$

where $E(m,n)$ indicates edge density at the pixel (m, n) and N_R indicates the number of pixel points in the candidate region.

The lane lines were identified by the maximum stable extreme value region (MSER) algorithm (Yang et al., 2016). This algorithm could filter many unpredictable noise regions, such as potholes and obstacles on the road. The method was used to perform a binarization operation for an image with a threshold. The connected regions the area of which rarely varied with the increase in the threshold were considered as MSERs.

$$u(i) = \frac{\left|Q_{i+\Delta} - Q_{i-\Delta}\right|}{\left|Q_i\right|} \tag{7}$$

where Q_i represents the area of the i^{th} connected region and Δ represents the slight variation in the threshold.

After the stable region of lane lines was obtained, the progressive probabilistic Hough transform (PPHT) algorithm (Elbayoumi et al., 2015) was introduced to identify the lane lines. Combining the identified license plate and the lane lines, it becomes possible to accurately determine the transverse position of the vehicle. This is achieved by analyzing the distance between the license plate and the lane lines within the image.

$$\frac{L_a}{D_a} = \frac{L_p}{D_p} \tag{8}$$

where L_a and L_p represent the actual distance and pixel distance between the lane lines, respectively, while D_a and D_p represent the actual distance and pixel distance between the license plate and the lane line, respectively.

Identification of Axles and Speed

We detected the axles of the vehicle using the lateral video. One could identify the wheels based on the standard Hough circle transform, which was similar to the line detection using Hough transform. The circle equation in the Cartesian coordinate was transformed into the Hough space and the following equation was obtained:

$$\begin{cases} a = x - r * \cos\theta \\ b = y - r * \sin\theta \end{cases} \tag{9}$$

The concyclic points were mapped as intersecting conical surfaces in the Hough space. Therefore, the points with the maximumt number of intersections represented the detected wheel.

Two auxiliary detection lines with known distance were drawn in the monitoring section on the deck to identify the vehicle's speed and wheelbase. The lane-line detection method was used to detect the auxiliary detection lines. The wheelbase of a vehicle could be estimated according to the positional relationship between the wheels and the auxiliary lines:

$$\frac{WL_a}{AL_a} = \frac{WL_p}{AL_p} \tag{10}$$

where WL_a indicats the vehicle's actual wheelbase, WL_p indicates the image's pixel distance and AL_a and AL_p indicate the actual distance and pixel distance between the two auxiliary detection lines, respectively.

Two different frame images were extracted when the vehicle passed through the monitoring section. One could identify the position of the same wheel in every frame image. Based on the distance Δ_s of the same wheel in the two frame images and the time interval Δ_t between the two frame images, the vehicle's speed could be evaluated as:

$$v = \frac{\Delta s}{\Delta t}. \quad (11)$$

EXPERIMENT IN THE LABORATORY

Experimental Model

A model experiment was performed in the laboratory to verify the proposed method. The model was a steel-box girder bridge with a length of 2.7m and a width of 0.83m. Two- and three-axle vehicles were built and their wheelbase could be changed. A leading beam and a tailing beam were installed on both ends of the main beam to ensure that the vehicle smoothly passed the box girder bridge (for simplicity, it was named the main beam), A motor was fixed at the end of the tailing beam to pull the vehicle through the main beam. We can adjust the vehicle's speed moving on the main beam by changing the belt pulley with different diameters. Two lane lines and auxiliary detection lines were drawn on the deck. The practice distance between two lane lines was 0.625m and that between two auxiliary lines was 1.2 m. One of the auxiliary lines was marked scale line as the criterion for comparing with the identified transverse position of the vehicle. One camera was installed in front of the main beam to monitor the frontal video and the other cameras were set on the sides of the main beam to capture the lateral video. Here, two common smart phones were used to monitor the video. The detailed experimental system is shown in Fig.2.

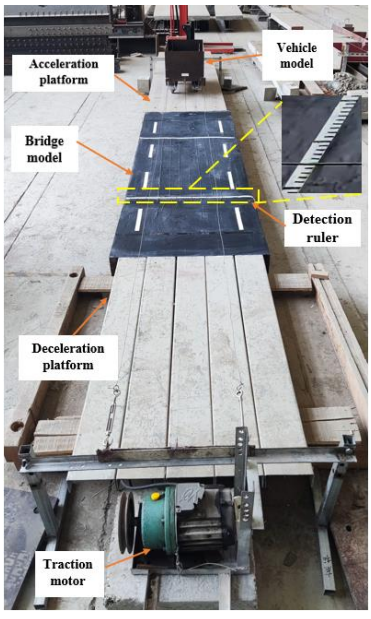

Figure (2): The experimental set-up of the steel-box girder bridge model

RESULTS

Multiple running tests pulled by the motor were performed by changing the type of the vehicle, the transverse position and the vehicle's speed. The video information was captured. First, the vehicle was detected and the license plate was identified. Then, the lane lines were identified based on the frontal video using the proposed method to locate the transverse position. One of the identified results is presented in Fig. 3.

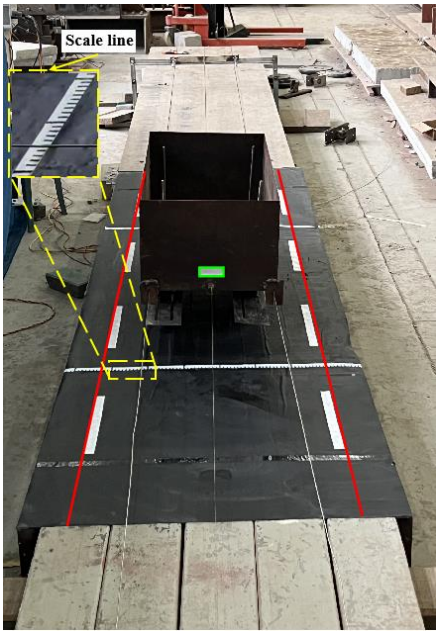

Figure (3): Location of the transverse position based on the frontal video

As illustrated in the figure, the identified lane line is denoted with a red line and the license plate is outlined with a green box. The scale line on the auxiliary line determined the actual transverse position of the vehicle, which was compared with the identified result.

Second, the proposed algorithm based on the lateral monitoring video was employed to identify the axles of the vehicle and the auxiliary lines. Then, the wheelbase and the vehicle's speed were estimated. The identified results are depicted in Fig. 4, where the identified wheel is marked with a blue circle and the auxiliary lines are marked by red lines.

Figure (4): Identification of the axles and vehicle's speed based on the lateral video

Two- and three-axle experimental vehicles were tested. Seven types of wheelbases were set for each vehicle and five lateral positions were set for each wheelbase for testing with different speeds. A total of 70 tests were carried out and then, the spatiotemporal information of the vehicle was obtained using the proposed method. Due to the limitation of space, here only the identification results of one transverse position for each wheelbase are listed in Tables 1 and 2. the statistical analysis results of all tests are presented in Table 3.

Table 1. Identified experimental result of the wheelbase of the vehicle

Vehicle type	Test ID	L1(cm)			L2(cm)		
		Actual value	Identified value	Absolute value of error (%)	Actual value	Identified value	Absolute value of Error (%)
2-axle	1	38	38.1	0.26	-	-	-
	2	43	43.1	0.23	-	-	-
	3	46	45.6	0.87	-	-	-
	4	49	48.5	1.02	-	-	-
	5	52	53	1.92	-	-	-
	6	55	54.6	0.73	-	-	-
	7	57	57.6	1.05	-	-	-
3-axle	8	20	20.3	1.50	45	44.6	0.89
	9	15	15.3	2.00	38.5	38.5	0.00
	10	19	18.5	2.63	34.5	34.8	0.87
	11	16	15.8	1.25	41	40.6	0.98
	12	13.5	13.1	2.96	37.5	37.4	0.27
	13	15.5	15.5	0.00	35	35.6	1.71
	14	21	21.1	0.48	36	35.6	1.11

Note: L1 is the wheelbase from the second axle to the first axle; L2 is the wheelbase from the third axle to the second axle.

Table 2. Identified experimental result of the transverse position and vehicle's speed

Test ID	Transverse position (cm)			Speed (cm/s)		
	Actual value	Identified value	Deviation (mm)	Actual value	Identified value	Absolute value of error (%)
1	14	14.2	2	12.8	12.67	1.02
2	31.5	31.2	3	20.5	20.2	1.46
3	35.1	35.2	1	35	35.4	1.14
4	33.2	33.1	1	30	30.8	2.67
5	33	33.2	2	40.5	40.9	0.99
6	28.6	28.9	3	35	34.2	2.29
7	36	36.5	5	20.5	20.1	1.95

8	26.5	26.2	3	18.5	18.72	1.19
9	34.7	34.2	5	30	30.5	1.67
10	34.1	34.5	4	35	35.6	1.71
11	31.8	31.8	0	40.5	40.9	0.99
12	24.6	24.8	2	35	35.4	1.14
13	18.5	18.4	1	45	45.6	1.33
14	37.6	37.5	1	45	44.2	1.78

Note: The error of the transverse position is defined as the percent of absolute value of the error *versus* the distance between two lane lines.

Table 3. Statistical results of identification error

Type	Wheelbase (%)	Deviation of transverse position (mm)	Speed (%)
Maximum	2.96	13	3.14
Mean	1.12	2.57	1.25
Variance	0.59	3.35	0.57

As depicted in the tables, the maximum identified deviation of the transverse position was 13 mm and the mean value of deviation was 2.57 mm. The maximum and mean value of identified error of the wheelbase were 2.96% and 1.12% and those of the vehicle's speed were 3.14% and 1.25%, respectively. The variances of identified error of the three parameters were 0.59%, 3.35 mm and 0.57%, respectively. The results verified the reliability and accuracy of the proposed method.

Field Tests

Some experiments were carried out on site to further verify the proposed method. One side of the road was selected as a testing section. This section comprised two lane lines with a distance of 3.3m between them. Two red cloth strips were fixed on the road with a distance of 7m as auxiliary detection lines, which were perpendicular to the lane lines. One of the auxiliary lines was marked scale line for locating exactly the transverse position of the vehicle. A mobile phone was fixed on the pedestrian bridge in front of the monitoring section to collect the frontal video and another mobile phone was fixed on the side of the road to capture the lateral video. One drove a car with two axles across the test road at different speeds from different transverse positions. The real-time videos were captured and the speed shown in the tachometer was recorded. A total of 24 tests were conducted.

Let us consider one test as an example. Initially, the vehicle was detected using the proposed background-difference technique. The original image is shown in Fig. 5(a) and the identified background image and vehicle are shown in Fig. 6(b) and Fig. 6(c), respectively.

(a) Original monitoring image

(b) Identified background image

(c) Detected vehicle

Figure (5): Vehicle detection results based on the background-difference technique

Next, the transverse position of the vehicle was located based on the proposed method. The identified result is illustrated in Fig.6. In the figure, the detected lane lines and license plate are marked with red and green lines, respectively.

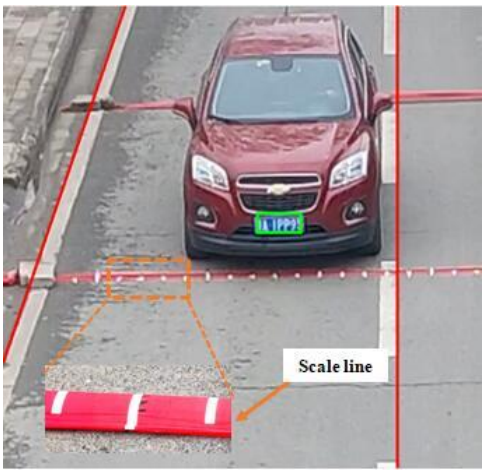

Figure (6): The location of the transverse position of the vehicle

We could identify the wheel and the auxiliary lines by capturing the lateral video. The analysis result is illustrated in Fig.7. The auxiliary lines and the wheel contour are marked with green lines and blue circles, respectively. Hence, the wheelbase and the vehicle's speed were calculated. Additionally, the speed displayed on the tachometer was captured for comparison with the identified result.

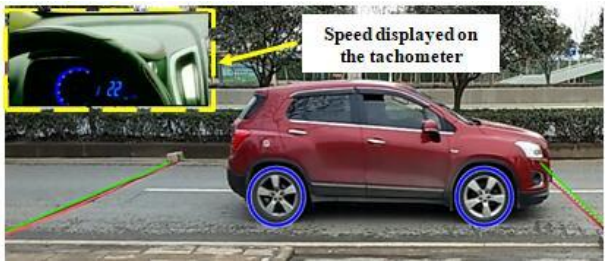

Figure (7): The identified result of the wheelbase and the vehicle's speed

The other field tests were performed at the other site with a different vehicle. The same test procedure was implemented 34 times with different speeds and transverse positions and one of the identified results was illustrated in Figs. 8 and 9.

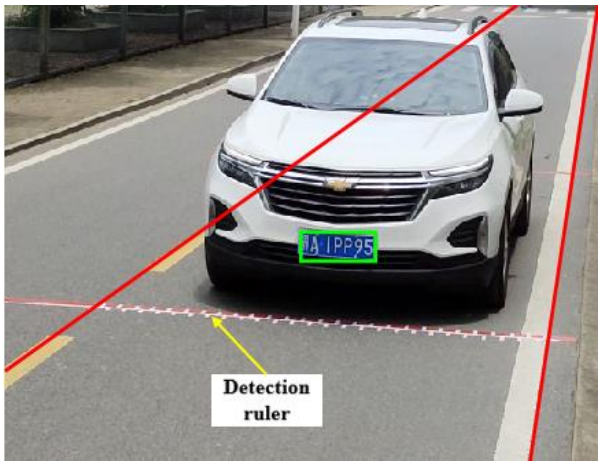

Figure (8): The identification of the transverse position of the vehicle

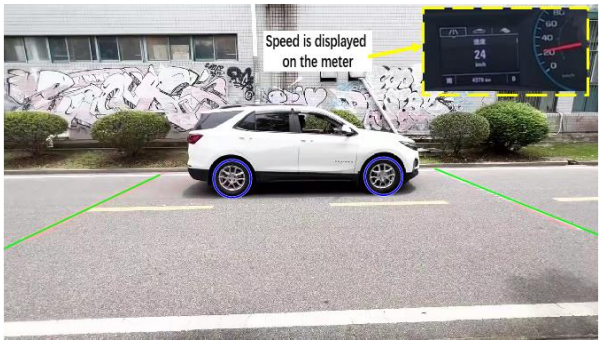

Figure (9): The identification of the wheelbase and the vehicle's speed

All the test data was collected and analyzed using the proposed algorithm. For the sake of space, the identified results of 10 tests for each site were listed in Table 4. The transverse position of the left outer lane line in Fig. 6 and 8 is defined as 0 and the error of the transverse position is defined as the absolute value of deviation. The actual value of the vehicle's speed was captured using the tachometer for compassion. The statistical analysis results of all tests are presented in Table 5.

Table 4. Identified results of the field test

Test ID	Transverse position (m)			Speed (km/h)			Wheelbase (m)		
	Actual value	Identified value	Deviation (cm)	Actual value	Identified value	Absolute value of error (%)	Actual value	Identified value	Absolute value of error (%)
1	1.8	1.82	2	18	17.5	-2.78	2.555	2.515	1.57
2	2.1	2.07	3	23	23.2	0.87	2.555	2.470	3.33
3	2.55	2.51	4	27	27.7	2.59	2.555	2.493	2.43
4	2.8	2.84	4	28	28.2	0.71	2.555	2.485	2.74
5	3	3.05	5	31	31.3	0.97	2.555	2.488	2.62
6	3.25	3.27	2	33	32.2	-2.42	2.555	2.533	0.86
7	3.8	3.77	3	37	37.8	2.16	2.555	2.515	1.57
8	3.95	3.9	5	42	42.5	1.19	2.555	2.558	0.12
9	4.2	4.15	5	47	46.6	-0.85	2.555	2.528	1.06
10	4.45	4.42	3	50	50.1	0.2	2.555	2.55	0.20
11	1.03	1.01	2	26	26.5	1.92	2.725	2.731	0.22
12	1.45	1.46	1	34	34.5	1.47	2.725	2.733	0.29
13	0.85	0.82	3	35	35.6	1.71	2.725	2.750	0.92
14	1	0.98	2	20	20.3	1.50	2.725	2.725	0.00
15	1.32	1.28	4	16	15.9	0.62	2.725	2.723	0.07
16	1.25	1.22	3	25	24.4	2.40	2.725	2.732	0.26
17	1.3	1.32	2	30	30.2	0.67	2.725	2.752	0.99
18	1.05	1.01	4	14	13.9	0.71	2.725	2.741	0.59
19	0.45	0.44	1	25	24.9	0.40	2.725	2.706	0.70
20	1.15	1.12	3	40	40.2	0.50	2.725	2.699	0.95

Table 5. Statistical results of identification error of field test

Type	Wheelbase (%)	Deviation of transverse position (cm)	Speed (%)
Maximum	3.33	5	2.78
Mean	1.12	2.69	1.35
Variance	0.78	1.83	0.54

As depicted in the tables, the maximum identified deviation of the transverse position was 5 cm and the average of deviation was 2.69 cm. The average and maximum of identified error of the wheelbase were 1.12% and 3.33% and those of the vehicle's speed were 1.35% and 2.78%, respectively. The variances of identified error of the three parameters were 0.78%, 1.83 cm and 0.54%, respectively. The field test achieved the same level of identified results as the model experiments, which further verified that the proposed method had good identification accuracy and reliability.

The above tests were conducted during daylight with good light. It is worth noting that the light was darker at night in practical environment. Fortunately, the proposed algorithm mainly identified some coarse targets, such as lane lines, license plate outline and wheels' outline, … etc. It needn't to focus on some details of the vehicle, which extended the application scenario of the proposed method. Figs. 10 and 11 present a practical application example at night.

Figure (10): The transverse location result of vehicle at night

Figure (11): The wheel detection results at night

It could be seen that the lane and license plate could be identified in the usual urban street lighting situation. If auxiliary detection lines were appropriately set, the spatiotemporal parameter could be obtained using the proposed method. Additionally, we also could add a light source in the monitoring section to improve the performance of the algorithm.

Another issue that needed attention in the practical operational environment was multi-vehicle scenarios (e.g. multiple vehicles in one or different lanes). We processed this problem as follow. Firstly, we would fix the camera's shooting angle to capture the traffic scene for determining section on the bridge. As shown in Fig. 12, the scene without any vehicle would be extracted as a background image. Based on the detected lane lines on the image, we could divide the background image into three separate parts corresponding to different lanes. In addition, a detection area was fixed in advance as marked with yellow lines. Only the vehicle entering the monitoring area was detected, as shown in Fig.13. Therefore, when a vehicle entered the detection area, the system will trigger the identification process. Every separate image only including the detected area was extracted for the following spatiotemporal information-identification of vehicle, which would ensure that there was one lane and a vehicle in the image to be analyzed. Until the vehicle left the monitoring area, the system would finish the identification process and is ready for next identification.

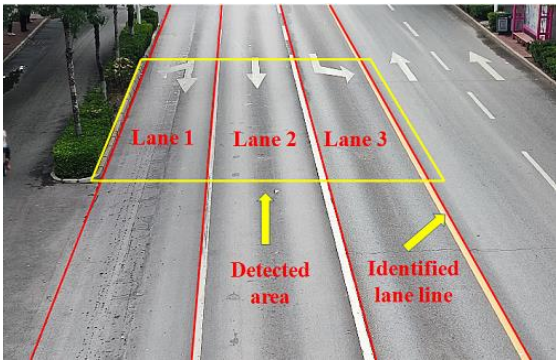

Figure (12): The separated background image with fixed detected area

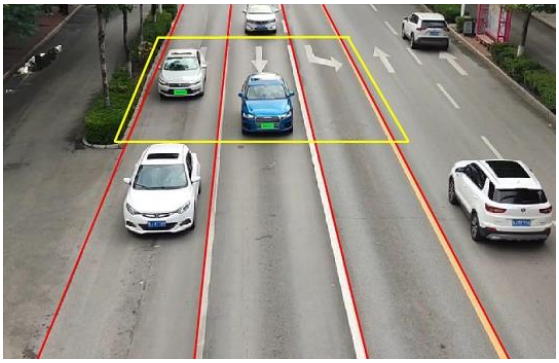

Figure (13): The vehicle detection under multi-vehicle scenarios

Certainly, when the quality of captured images was poor; for example, blurry images obtained in foggy weather, smeared image with shadow at night when the streetlights were dim or imprecise images where the target vehicle was shielded by other vehicles due to heavy traffic flow, the proposed machine-vision method may not be able to detect license plates and wheels and spatiotemporal locating couldn't be achieved.

CONCLUSIONS

A machine-vision method was proposed to identify the spatiotemporal information of the vehicle in this study. Numerous laboratory scaled-down model experiments and field tests were carried out and statistic

analyses were performed to verify the proposed method. The identified results indicated that:

(1) The average deviation of the transverse position was 2.57mm for laboratory experiments and 2.69 cm for field tests. Therefore, the lateral-positioning precision was high.
(2) The average identification errors of wheelbase for both laboratory experiment and field test were 1.12% and those of the vehicle's speed were 1.25% for laboratory and 1.35% for field test. This verified the effectiveness and accuracy of the proposed method.
(3) The variances of identified error of the three parameters for model experiment were 0.59%, 3.35 mm and 0.57%, respectively. For the field test, they were 0.78%, 1.83 cm and 0.54%, respectively. This verified the reliability of the proposed algorithm.
(4) Preliminary analysis indicated lane lines, license plate outline and wheels' outline could be identified using the proposed algorithm in the night environment, which validated the anti-noise performance of the proposed method.
(5) Identification of spatiotemporal information of vehicle loads was very important for understanding the exact loading conditions and behaviors of bridges. Combined with strain data measured by a small number of strain sensors, the axle and total weight of vehicle could be further identified. This was an effective and low-cost technique to obtain vehicle loads' information on bridges.
(6) The machine-vision technique did not need to install sensors on the road; only the cameras need to be installed, which was convenient and fast for engineering applications, especially for bridges that have been installed with a structural health-monitoring system including cameras and strain sensors. The use of the proposed method was expected to expand the functions of the existing health-monitoring system without incremental costs.

Acknowledgments

This research is financially supported by the National Natural Science Foundation of China (Grant No. 51408250) and the Hubei University of Technology Postgraduate Innovative Talent Training Program (Grant No. Univ. 2022054). The authors would also like to thank the reviewers for their suggestions which contributed to improve this manuscript.

REFERENCES

Brown, R., and Wicks, A.L. (2016). "Vehicle-tracking for bridge load dynamics using vision techniques". Structural Health Monitoring, Damage Detection & Mechatronics, 7, 83-90.

Chen, A.R., Ma, R.J., and Xu, Y.M. (2013). "Vehicle-loading identification and its characteristics of Sutong bridge in operation". Journal of Chong Qing JiaoTong University (Natural Science), 32 (9), 729-733.

Chen, Z., Li, H., Bao, Y., Li, N., and Jin, Y. (2016). "Identification of spatio-temporal distribution of vehicle loads on long-span bridges using computer-vision technology". Structural Control and Health Monitoring, 23, 517 - 534.

Deng, L., He, W., Yu, Y., and Cai, C.S. (2018). "Equivalent shear-force method for detecting the speed and axles of moving vehicles on bridges". Journal of Bridge Engineering, 23(8), 04018057.

ElBayoumiHarb, S.M., Isa, N.A.M., and Salamah, S.A. (2015). "Improved image-magnification algorithm based on Otsu thresholding". Computers & Electrical Engineering, 46, 338-355.

Han, W., Liu, X., Gao, G., Xie, Q., and Yuan, Y. (2018). "Site-specific extra-heavy truck load characteristics and bridge-safety assessment". Journal of Aerospace Engineering, 31 (6), 04018098.

He, W., Ling, T., O'brien, E.J., and Deng, L. (2019). "Virtual-axle method for bridge weigh-in-motion systems requiring no axle detector". Journal of Bridge Engineering, 24 (9), 04019086.

Jia, Z., Fu, K., and Lin, M. (2019). "Tire-pavement contact-aware weight estimation for multi-sensor WIM systems". Sensors, 19 (9), 2027.

Jiang, X., Liu, Z., Liu, B., and Liu, J. (2022). "Multi-sensor fusion for lateral vehicle localization in tunnels". Applied Sciences, 12, 6634.

Khuc, T., and Catbas, F.N. (2018). "Structural identification using computer vision-based bridge health monitoring". Journal of Structural Engineering-ASCE, 144, 04017202.

Kim, S., Lee, J., Park, M.S., and Jo, B.W. (2009). "Vehicle signal analysis using artificial neural networks for a bridge weigh-in-motion system". Sensors, 9 (10), 7943-7956.

Li, C.-Y., Wang, C., Yang, Q.X., and Qi, T.Y. (2022). "Identification of vehicle loads on an orthotropic-deck steel-box beam bridge based on optimal combined strain influence lines". Applied Sciences, 12 (19), 9848.

Li, D, Nie J.H., Ren, W.X, Ng, W.H., Wang, G.H., and Wang, Y. (2022). "A novel acoustic emission source-location method for crack monitoring of orthotropic steel plates". Engineering Structures, 253, 113717.

Miao, B.R., Zhou, F., Jiang, C., Chen, X., and Yang, S. (2018). "A comparative study of regularization method in structure-load identification". Shock and Vibration, 9204865.

Obaidat, M.T. (2020). "Cellular-phone-based system for transportation engineering applications". Alexandria Engineering Journal, 59, 1197-1204.

Obaidat, M.T., Al-Masaeid, H.R., Al-Haji, O., and Qudah, A.M. (2007). "A knowledge-based system for pedestrian's roadway crossing behavior through video cameras". Jordan Journal of Civil Engineering, 1.

Obaidat, M.T., and Tasneem, K.H. (2022). "Potential of computer-vision cellular-phone based system to extract traffic parameters". Information Sciences Letters, 11 (3), 817 - 826.

OBrien, E.J., and Enright, B. (2013). "Using weigh-in-motion data to determine aggressiveness of traffic for bridge loading". Journal of Bridge Engineering, 18 (3), 232-239.

Sujon, M., and Dai, F. (2021). "Application of weigh-in-motion technologies for pavement-and bridge-response monitoring: State-of-the-art review". Automation in Construction, 130, 103844.

Wang, H., Wang, Q., Zhai, J., Yuan, D., Zhang, W., Xie, X., Zhou, B., Cai, J., and Lei, Y. (2022). "Design of fast-acquisition system and analysis of geometric features for highway tunnel lining cracks based on machine vision". Applied Sciences, 12, 2516.

Wang, N.-B., Ren, W.-X., and He, W.-Y. (2013). "Wavelet-transform method for identification of vehicle axles on a bridge". Journal of Vibration Engineering, 26(4), 539-544.

Wu, T., Zhang, L., Wen, J., and Ni, Z. (2021). "Influence of common factors on vehicle bridge coupling vibration". Procedia-Vibroengineering, 36, 60-65.

Xiao, Z., Yamada, K., Inoue, J., and Yamaguchi, K. (2006). "Measurement of truck axle weights by instrumenting longitudinal ribs of orthotropic bridge". Journal of Bridge Engineering, 11 (5), 526-532.

Yamaguchi, E., Kawamura, S.-I., Matuso, K., Matsuki, Y., and Naito, Y. (2009). "Bridge-weigh-in-motion by two-span continuous bridge with skew and heavy-truck flow in Fukuoka area, Japan". Advances in Structural Engineering, 12 (1), 115-125.

Yang, G., Chen, W., and Xu, J. (2012). "The theory and case study of axle-load identification based on BWIM of orthotropic steel deck". Applied Mechanics and Materials, 204-208, 1247-1254.

Yang, H., Yan, W.M., and He, H. (2016). "Parameters identification of moving load using ANN and dynamic strain". Shock and Vibration, 2016, 1-13.

Zhang, B., Zhou, L., and Zhang, J. (2019). "A methodology for obtaining spatiotemporal information of the vehicles on bridges based on computer vision". Computer-aided Civil and Infrastructure Engineering, 34 (6), 471-487.

Zhao, D., He, W., Deng, L., Wu, Y., Xie, H., and Dai, J. (2021). "Trajectory tracking and load monitoring for moving vehicles on bridge based on axle position and dual-camera vision". Remote. Sensing, 13, 4868.

Zhao, H., Tan, C.J., Zhang, L.W., and Qiao, D.Q. (2016). "Improved identification of vehicular axles in BWIM system based on wavelet transform". Journal of Hunan University Natural Sciences, 43, 111-119. 10.16339.

Zhao, Q., L. Wang, K. Zhao, and H. Yang. (2019). "Development of a novel piezoelectric sensing system for pavement dynamic-load identification". Sensors, 19 (21), 4668.

Zhou Z. (2013). "Application of BP neural networks to weigh-in-motion of vehicles". AASRI Winter International Conference on Engineering and Technology (AASRI-WIET 2013), Atlantis Press, 2013, 170-172.

Zhou, Y., Pei, Y., Ziwei, L., Fang, L., Zhao, Y., and Yi, W. (2020). "Vehicle-weight identification system for spatiotemporal load distribution on bridges based on non-contact machine-vision technology and deep-learning algorithms". Measurement, 159, 107801.

Zhu, J.H., Wang, C., Qi, T.Y., and Zhou, Z.S. (2022). "Vehicle load identification on orthotropic steel-box beam bridge based on the strain-response area". Applied Sciences, 12(23), 12394.

Zhu, Y., Sekiya, H., Okatani, T., Yoshida, I., and Hirano, S. (2022). "Real-time vehicle identification using two-step LSTM method for acceleration-based bridge weigh-in-motion system". Journal of Civil Structural Health Monitoring, 12, 689-703.